Molecular Electronics

DOI: 10.1002/anie.201309506

Dependency of the Tunneling Decay Coefficient in Molecular Tunneling Junctions on the Topography of the Bottom Electrodes**

*Li Yuan, Li Jiang, Bo Zhang, and Christian A. Nijhuis**

Abstract: *A controversy in molecular electronics is the unexplained large spread in values of the tunneling decay coefficient β in tunneling junctions with self-assembled monolayers of n-alkanethiolates (SC_n). We show control of the β value over the range 0.4–1.0 n_C^{-1} in junctions by changing the topography of the bottom electrodes that support the SAMs. Very low β values (0.4–0.5 n_C^{-1}) are obtained for rough surfaces with large areas of exposed grain boundaries, while $\beta = 1.0\ n_C^{-1}$ for smooth surfaces with small areas of exposed grain boundaries.*

The electrical characteristics of molecular electronic devices based on self-assembled monolayers (SAMs) are ideally determined by the properties of the molecular component and not by the electrodes or the molecule–electrode interfaces. The electrical characteristics of junctions with SAMs of *n*-alkanethiolates ($S(CH_2)_{n-1}CH_3 \equiv SC_n$) vary dramatically across test beds. A large number of studies have observed that the current density J ($A\,cm^{-2}$) decays exponentially with increasing SAM thickness d (n_C), but do so with a great variation in the so-called tunneling decay coefficient β of 0.4–1.1 n_C^{-1}.[1] The origin of the large spread of β values has been a major concern because without a good understanding of the factors that cause variations in the tunneling characteristics, it is difficult to interpret and compare data obtained from different test beds and to establish standards in the field.[2]

The most commonly used approach to model charge transport across these SAM-based junctions is with a simplified form of the Simmons equation [Eq. (1)],[3] where J_0

$$J = J_0 e^{-\beta d} \quad (1)$$

($A\,cm^{-2}$) is a constant that depends on the system and includes, for example, contact resistance.

A value of β close to 1.0 n_C^{-1} has been measured across many test beds and, thus, this value has become the empirical consensus value, but a large number of reports describe low values of β in the range 0.4–0.7 n_C^{-1}.[4] To account for the discrepancies in the parameter β, several models have been proposed, including rounding of the tunneling barrier by image charges,[4b] electrostriction (for junctions with Hg-drop top electrodes),[4a] deformation of the SAMs,[5] and changes in the mechanism of charge transport (chain-to-chain[6] versus through-bond tunneling[7]). A few research groups have related low β values to defects in the SAMs. Haiss et al.[4c] reported a β value of 0.60 n_C^{-1} for junctions formed at defect sites of the bottom electrode when using a scanning probe as a top electrode. Vilan and co-workers[8] showed for junctions based on SAMs of alkyl phosphonates on AlO_x electrodes contacted with Hg drops that the value of β depends on the length of the SAMs: short SAMs with $n = 8$, 10, or 12 had $\beta = 1.34 \pm 0.004\ n_C^{-1}$, while long SAMs with $n = 12$, 14, or 16 had $\beta = 0.77 \pm 0.05\ n_C^{-1}$ as a result of the presence of pin holes. Junctions with top electrodes of conductive polymers[4b] or graphene (and derivatives thereof)[4e] resulted in low values of β in the range 0.5–0.7 n_C^{-1}; however similar junctions but with a different conductive polymer[9] or graphene derivative[10] resulted in β values close to 1.0 n_C^{-1}. Despite the fact that the same SAMs have been tested across a large number of (similar) test beds, the origin of the large spread in β values is unclear.

Here we describe that a large range of values of β from 0.41 to 1.0 n_C^{-1} (which spans the entire range of values of β reported in the literature except for very high values of β[11]) can be obtained in a single test bed by changing the topography of the bottom electrode. We found that the fraction of the surface area covered by the grain boundaries is crucial, which is determined by the grain size (A_{gr}, nm^2) and the distance between neighboring grains (d_{gb}, nm). Surfaces with small grains contain large numbers of grain boundaries at which SAMs cannot pack well, which will be even worse for surfaces with large d_{gb} values. The root-mean-square (rms) roughness is large for surfaces where the grains are out of the plane with respect to each other, thereby resulting in even larger exposed areas of grain boundaries.

Figure 1 shows a typical AFM image of a bottom electrode which contains grains and grain boundaries. A part of the junction with a grain boundary is also shown schematically. SAMs cannot pack well at the grain boundaries and this results in defects inside the junctions. According to Equation (1), defects that lower the value of d (or thin-area defects) induce disorder in the SAMs, thereby resulting in high values of J, and a small fraction of thin-area defects in the junctions may dominate the electrical characteristics.[1c,12] Defects that increase the value of d (or thick-area defects) cause low values of J and are mainly the result of physisorbed

[*] L. Yuan, L. Jiang, B. Zhang, Prof. C. A. Nijhuis
Department of Chemistry, National University of Singapore
3 Science Drive 3, Singapore, 117543 (Singapore)
and
Graphene Research Centre, National University of Singapore
6 Science Drive 2, Singapore, 117546 (Singapore)
E-mail: chmnca@nus.edu.sg
Homepage: http://staff.science.nus.edu.sg/~christiannijhuis/index.html

[**] The Singapore National Research Foundation (NRF Award No. NRF-RF2010-03 to C.A.N.) is kindly acknowledged for supporting this research.

Supporting information for this article is available on the WWW under http://dx.doi.org/10.1002/anie.201309506.

 © 2014 Wiley-VCH Verlag GmbH & Co. KGaA, Weinheim

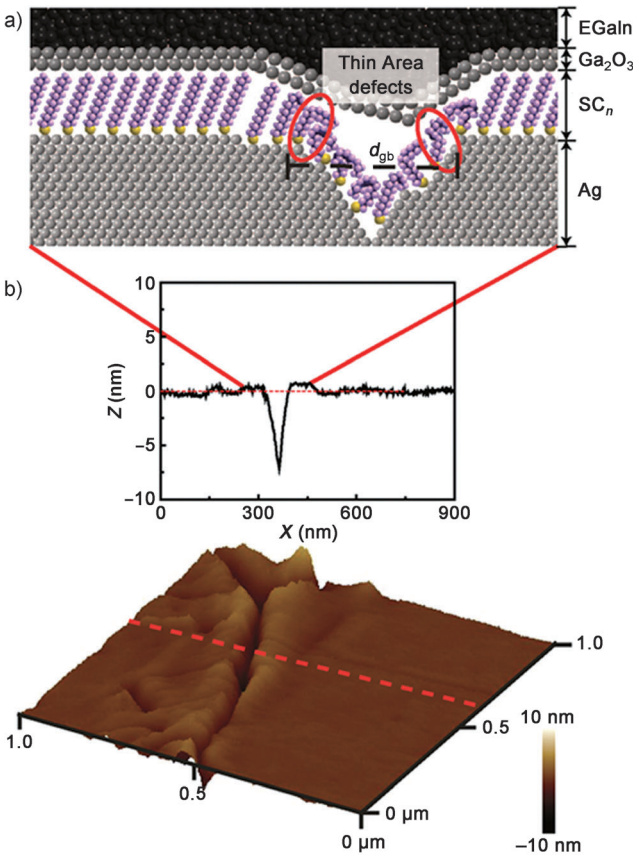

Figure 1. a) Schematic illustration of a junction with a SC_{14} SAM at a defect site induced by a grain boundary with a width d_{gb} (see main text). b) An AFM image of a $Ag^{A\text{-}TS}$ surface and a line scan. The red dashed line indicates the position of the line scan.

materials, or nonconformal contact of the electrode with the SAMs, but only scale with area.

To study the effect of the surface topography of the bottom electrode on the electrical characteristics of the junctions we fabricated eight different electrodes with a broad range of rms values (0.55–5.78 nm), A_{gr} values (9.45×10^2–9.07×10^5 nm^2), and d_{gb} values (27–130 nm) by four different methods (see the Supporting Information): 1) direct evaporation (DE) on Si/SiO_2 wafers,[13] 2) template stripping (TS),[14] 3) a combination of annealing and template stripping (A-TS), and 4) seeded growth (SD; seed layers of 2.0 nm of Ge or Ti were used for Ag and Au, respectively). These methods yield surfaces with a large dynamic range of surface properties and represent surfaces widely used in nanoelectronics (see Table S1 in the Supporting Information). Figure 2 shows the AFM images (and Table S4 in the Supporting Information summarizes the properties) of all the surfaces used in this study. To count the number of grains N_{gr} and to determine A_{gr} of the irregularly shaped grains, we analyzed the AFM images manually (see the Supporting Information). The values of d_{gb} (from 15 line-scans) and the rms values over an area of 1.0×1.0 μm^2 were determined using NanoScope Analysis 1.40. We estimated the fraction of the grain boundary area A_{gb} (nm^2) for each surface from the values of A_{gr} and d_{gb} (see the Supporting Information). To capture these parameters in a single parameter for the surface topography, we determined the bearing volume (BV, nm^3) by normalizing each sample for N_{gr} and using Equation (2):

$$BV = N_{gr} A_{gb} \text{ rms} \quad (2)$$

Thus, the parameter BV contains all the relevant information regarding the topography of the surface, and small BV values indicate that only a small fraction of the surface is dominated by grain boundaries, while the opposite is true for large BV values. We note that the BV value is different from that obtained with AFM analysis software, which depends on arbitrary chosen threshold values and on the volume of the voids between the grains (see the Supporting Information).

We determined the value of β using SAMs of SC_n (with $n=10$, 12, 14, 16, and 18) immobilized on these bottom electrodes and contacted them electrically with GaO_x/EGaIn top electrodes by using previously reported procedures (see the Supporting Information).[15] Figure 3 shows the histograms of all the currents measured at −0.50 V for Ag^{TS}-SC_n//GaO_x/EGaIn junctions to which we fitted Gaussians to obtain the log-mean (μ_{log}) of the value of J and the log-standard deviation value (σ_{log}). We repeated this procedure for all the applied biases to construct the log(average J(V)) curves (Figure 3b). In total, we used 19593 J(V) curves in our analysis (see Table S6 in the Supporting Information) to construct J versus n_C plots for each type of junction (Figure 3c,d; the data points are off-set in n_c by −0.2 for Ag^{TS} and Au^{TS}, and +0.2 for Ag^{DE2} and Au^{DE}, for clarity). (Table S6 in the Supporting Information summarizes the values of β and J_0 that were obtained by fitting the data to Equation (1)). We note that the current densities reported here are very similar to previously reported values.[1c,15]

Figure 4 shows the values of β as a function of BV and shows three distinct regimes (the dashed lines serve only as guides to the eye). 1) The value of β saturates at a value close to $1.0\ n_C^{-1}$ for very smooth TS and A-TS surfaces with the largest values of A_{gr} (ca. 30 and 800 times larger than Ag^{DE2} and Ag^{SD} surfaces, respectively) despite intermediate rms and d_{gb} values. 2) The value of β decreases with decreasing A_{gr} despite the lowest rms and d_{gb} values for SD surfaces. 3) The value of β reaches a lower limit at 0.40–0.50 n_C^{-1} for very rough DE surfaces (largest rms and d_{gb} values) despite an intermediate A_{gr} value. These results show that variations in the surface topography explain the spread in values of β and that the most important factor is the amount of exposed grain boundaries. Most studies have used electrodes prepared by DE or SD methods, but they are inferior to TS surfaces because of the large numbers of grains and grain boundaries. Similarly, Au surfaces always have larger BV values than the corresponding Ag surfaces and, therefore, result in lower β values, although the difference in tilt angle for SAMs on Ag (ca. 10°) and Au (ca. 30°) may also be in part responsible.[16] Remarkably, the yield of nonshorting junctions was (nearly) independent of the topography of the surface (Figure 4).

Figure 3 shows that the values of J for junctions with SAMs of SC_{10} are independent of the topography of the surface, from which we conclude that the effective electrical contact area[18] is constant. The current varied almost two

© 2014 Wiley-VCH Verlag GmbH & Co. KGaA, Weinheim

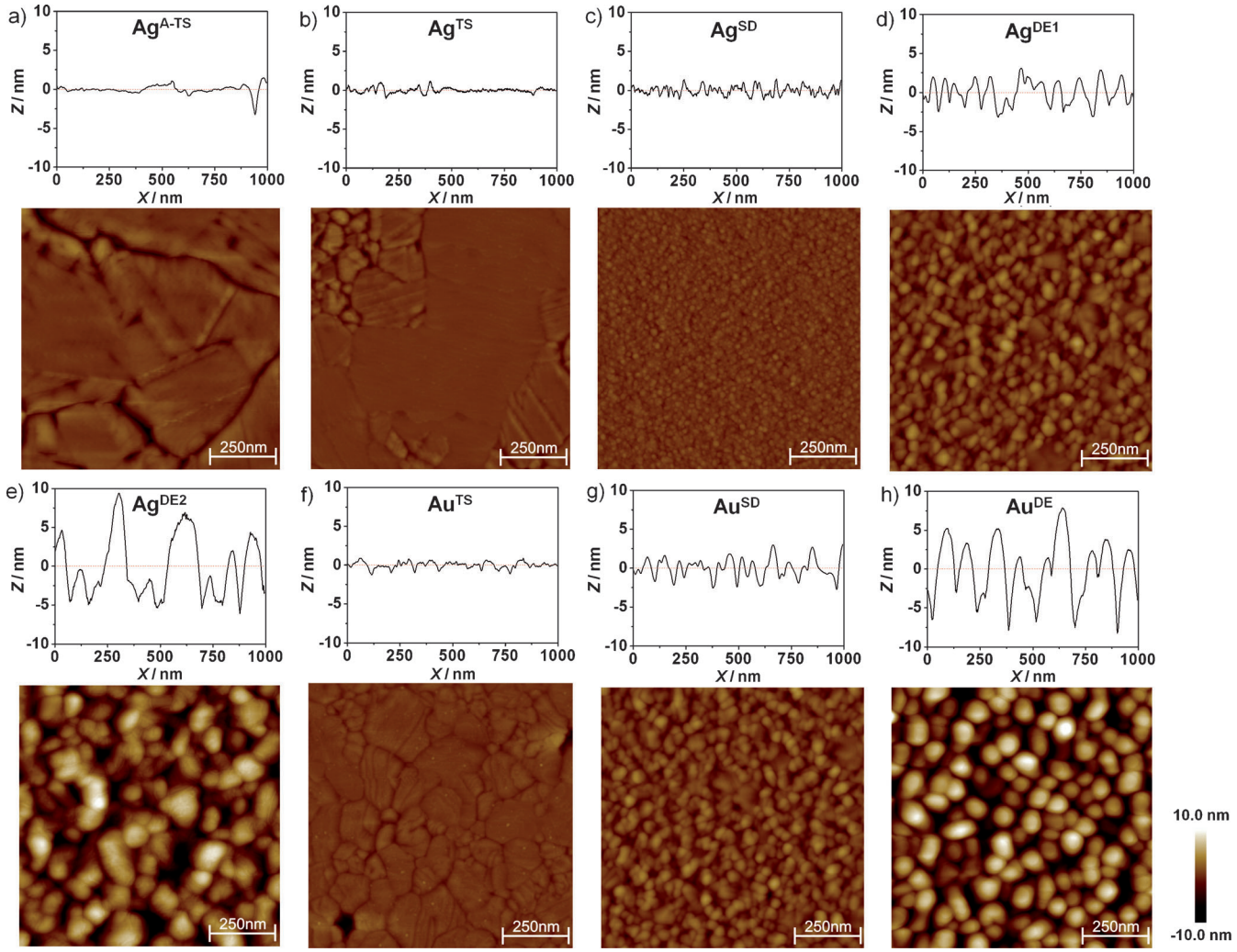

Figure 2. The AFM images ($1 \times 1\ \mu m^2$) and their corresponding line scans of the bottom electrodes fabricated by annealed template stripping of Ag (a), template stripping of Ag (b), Ge-seeded evaporation of Ag (c), direct evaporation of Ag with rms = 1.35 nm (d) or rms = 5.78 nm (e), template stripping of Au (f), Ti-seeded evaporation of Au (g), and direct evaporation of Au (h).

orders of magnitude for junctions with SAMs of SC_{18} (see Figures S7–S14 in the Supporting Information for all J(V) curves), from which we conclude that defects in the SAMs induced by grain boundaries are responsible for lowering the values of β (see the Supporting Information for a more detailed discussion). The van der Waals interactions between neighboring alkyl chains in SC_{10} SAMs are weaker than in SC_{18} SAMs. Consequently, SAMs of SC_{10} are loosely packed and liquid-like,[12,16,17] and can compensate for, and smoothen, thin-area defects.[8] The SAMs of SC_{18} yield densely packed films with near crystalline structure on flat grains and, therefore, cannot pack well at grain boundaries and contain more thin-area defects[12,16] than the more liquid-like SC_{10} SAMs. Hence, for SAMs on electrodes with small BV values, the assumption $d = n_C$ holds and leads to $\beta = 1.0\ n_C^{-1}$, while in the case of large BV values, d is smaller than n_C (because of thin area defects) and results in small values of β. A similar explanation has also been used by Vilan and co-workers[8] to account for the chain-length dependence of β for SAMs of alkyl phosphonates on AlO_x electrodes.

In conclusion, our results show that the Simmons Equation does not account for the subtle differences in SAM structures and inherent to the type of analysis—plotting the values of J for a given voltage against n_C^{-1} rather against the effective thickness of the SAM result in an overestimation of the SAM thickness and consequently an underestimation of the value of β. We controlled the value of β from 0.41 to $1.0\ n_C^{-1}$ by varying the BV of the bottom electrode without affecting the yield of nonshorting junctions. Thus, the observation of an exponential decay of the current as a function of the SAM thickness in combination with high yields in working devices is not sufficient to justify any conclusions regarding the quality of the junctions or the correctness of the value of β.

Our data also reveal that the value of J for junctions incorporating thin, liquid-like SAMs is insensitive to the topography of the bottom electrodes, in sharp contrast to thick crystalline SAMs. This liquid-like character of thin SAMs may also mask other properties of the SAMs and their effect on the charge-transport characteristics. For example,

 © 2014 Wiley-VCH Verlag GmbH & Co. KGaA, Weinheim

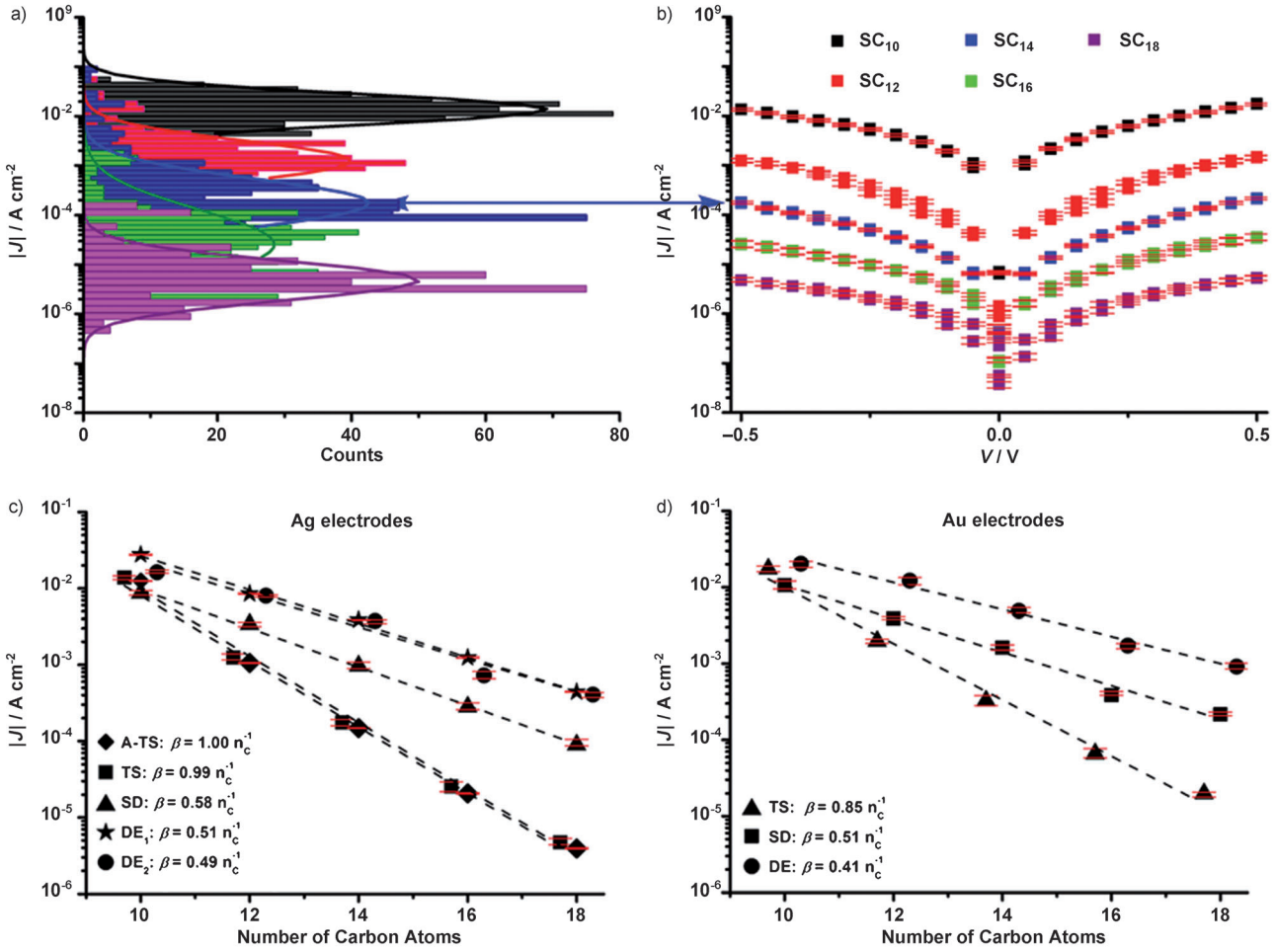

Figure 3. a) The histograms of $|J|$ at −0.50 V with Gaussian fits for Ag^{TS}-SC_n//Ga_2O_3/EGaIn junctions (n = 10(−), 12(−), 14(−), 16(−), or 18(−)). b) Plots of the log(average J(V)) curves for Ag^{TS}-SC_n//Ga_2O_3/EGaIn junctions. Plots of log $|J|$ at −0.50 V versus n_C for junctions incorporating SAMs on Ag (c) and Au (d) substrates. The dashed lines are fits to Equation (1). All error bars (−) represent 95% confidence intervals. To avoid overlapping data points, we off-set n_C by −0.2 for the Ag^{TS} and Au^{TS} surfaces, and +0.2 for the Ag^{DE2} and Au^{DE} surfaces.

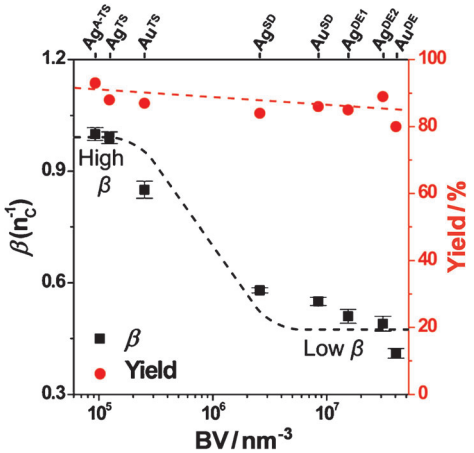

Figure 4. Plot of β and yield against BV. The dashed lines (in red and black) are guides to the eye.

Yoon et al.[19] and Sayed et al.[20] found that the electrical properties of junctions with thin SAMs were independent of a large variety in functional head groups. We showed that decreasing the packing energy of SAMs by only 0.5 kcal mol^{-1} was sufficient to mask the presence of ferrocene head groups (the mismatch in head group size and alkyl chain diameter also induces liquid-like behavior[16]). The results described here help to explain the large spread of β values reported across many test beds and the importance of understanding the role of disorder in the SAMs in the electrical characteristic of SAM-based junctions.

Received: November 1, 2013
Published online: February 25, 2014

Keywords: bottom electrodes · charge transport · molecular electronics · self-assembled monolayers · tunneling decay constant

[1] a) A. Salomon, D. Cahen, S. Lindsay, J. Tomfohr, V. B. Engelkes, C. D. Frisbie, *Adv. Mater.* **2003**, *15*, 1881 – 1890; b) H. B. Akkerman, B. de Boer, *J. Phys. Condens. Matter* **2008**, *20*, 013001; c) C. A. Nijhuis, W. F. Reus, J. R. Barber, G. M. Whitesides, *J. Phys. Chem. C* **2012**, *116*, 14139 – 14150.
[2] R. L. McCreery, A. J. Bergren, *Adv. Mater.* **2009**, *21*, 4303 – 4322.

 © 2014 Wiley-VCH Verlag GmbH & Co. KGaA, Weinheim

[3] J. G. Simmons, *J. Appl. Phys.* **1963**, *34*, 1793 – 1803.
[4] a) Y. Selzer, A. Salomon, D. Cahen, *J. Phys. Chem. B* **2002**, *106*, 10432 – 10439; b) H. B. Akkerman, R. C. G. Naber, B. Jongbloed, P. A. van Hal, P. W. M. Blom, D. M. de Leeuw, B. de Boer, *Proc. Natl. Acad. Sci. USA* **2007**, *104*, 11161 – 11166; c) W. Haiss, S. Martin, E. Leary, H. van Zalinge, S. J. Higgins, L. Bouffier, R. J. Nichols, *J. Phys. Chem. C* **2009**, *113*, 5823 – 5833; d) A. B. Neuhausen, A. Hosseini, J. A. Sulpizio, C. E. D. Chidsey, D. Goldhaber-Gordon, *Acs Nano* **2012**, *6*, 9920 – 9931; e) T. Li, J. R. Hauptmann, Z. M. Wei, S. Petersen, N. Bovet, T. Vosch, J. Nygård, W. P. Hu, Y. Q. Liu, T. Bjørnholm, K. Nørgaard, B. W. Laursen, *Adv. Mater.* **2012**, *24*, 1333 – 1339.
[5] X. D. Cui, X. Zarate, J. Tomfohr, O. F. Sankey, A. Primak, A. L. Moore, T. A. Moore, D. Gust, G. Harris, S. M. Lindsay, *Nanotechnology* **2002**, *13*, 5 – 14.
[6] H. Song, H. Lee, T. Lee, *J. Am. Chem. Soc.* **2007**, *129*, 3806 – 3807.
[7] K. Slowinski, R. V. Chamberlain II, R. Bilewicz, M. Majda, *J. Am. Chem. Soc.* **1996**, *118*, 4709 – 4710.
[8] I. Levine, S. M. Weber, Y. Feldman, T. Bendikov, H. Cohen, D. Cahen, A. Vilan, *Langmuir* **2012**, *28*, 404 – 415.
[9] F. Milani, C. Grave, V. Ferri, P. Samorì, M. A. Rampi, *ChemPhysChem* **2007**, *8*, 515 – 518.
[10] G. Wang, Y. Kim, M. Choe, T. W. Kim, T. Lee, *Adv. Mater.* **2011**, *23*, 755 – 756.
[11] K. Slowinski, M. Majda, *J. Electroanal. Chem.* **2000**, *491*, 139 – 147.
[12] E. A. Weiss, R. C. Chiechi, G. K. Kaufman, J. K. Kriebel, Z. F. Li, M. Duati, M. A. Rampi, G. M. Whitesides, *J. Am. Chem. Soc.* **2007**, *129*, 4336 – 4349.
[13] T. Sawaki, Shinku-Jyochaku, *Vacuum Evaporation*, Nikkan Kogyo Shinbun, Tokyo Japan, **1969**.
[14] N. Nerngchamnong, L. Yuan, D. C. Qi, J. Li, D. Thompson, C. A. Nijhuis, *Nat. Nanotechnol.* **2013**, *8*, 113 – 118.
[15] W. F. Reus, C. A. Nijhuis, J. R. Barber, M. M. Thuo, S. Tricard, G. M. Whitesides, *J. Phys. Chem. C* **2012**, *116*, 6714 – 6733.
[16] J. C. Love, L. A. Estroff, J. K. Kriebel, R. G. Nuzzo, G. M. Whitesides, *Chem. Rev.* **2005**, *105*, 1103 – 1169.
[17] P. E. Laibinis, M. A. Fox, J. P. Folkers, G. M. Whitesides, *Langmuir* **1991**, *7*, 3167 – 3173.
[18] F. C. Simeone, H. J. Yoon, M. M. Thuo, J. R. Barber, B. Smith, G. M. Whitesides, *J. Am. Chem. Soc.* **2013**, *135*, 18131 – 18144.
[19] H. J. Yoon, N. D. Shapiro, K. M. Park, M. M. Thuo, S. Soh, G. M. Whitesides, *Angew. Chem.* **2012**, *124*, 4736 – 4739; *Angew. Chem. Int. Ed.* **2012**, *51*, 4658 – 4661.
[20] S. Y. Sayed, A. Bayat, M. Kondratenko, Y. Leroux, P. Hapiot, R. L. McCreery, *J. Am. Chem. Soc.* **2013**, *135*, 12972 – 12975.

 © 2014 Wiley-VCH Verlag GmbH & Co. KGaA, Weinheim